

Atty. Dkt. No. 060925-1900

UNITED STATES PATENT AND TRADEMARK OFFICE

Applicant: H. Michael SHEPARD
Title: METHODS TO TREAT
AUTOIMMUNE AND
INFLAMMATORY CONDITIONS
Appl. No.: 10/051,320
Filing Date: January 18, 2002
Examiner: Kim, Jennifer M.
Art Unit: 1617

<p>CERTIFICATE OF MAILING I hereby certify that this correspondence is being deposited with the United States Postal Service with sufficient postage as First Class Mail in an envelope addressed to: Mail Stop AF, Commissioner for Patents, P.O. Box 1450, Alexandria, VA 22313-1450, on the date below.</p> <p>_____ Esther Lily C. Esguerra (Printed Name)</p> <p>_____ (Signature)</p> <p>_____ December 27, 2005 (Date of Deposit)</p>

DECLARATION OF H. MICHAEL SHEPARD UNDER 37 C.F.R. § 1.132

Mail Stop AF
Commissioner for Patents
P.O. Box 1450
Alexandria, VA 22313-1450

Sir:

I, H. Michael Shepard, hereby declare as follows:

1. I am the H. Michael Shepard who is named as the inventor of the above-identified application.
2. I am the same H. Michael Shepard who is named as a co-author of the journal article entitled "Enzyme-catalyzed therapeutic agent (ECTA) design: activation of the antitumor ECTA compound NB1011 by thymidylate synthase" that appeared in Biochemical Pharmacology 61:179-189 (2001). A copy of this article is attached to this Declaration.

3. My co-authors for the attached article did not contribute to the invention disclosed and claimed in this application. The subject application relates to the treatment of autoimmune disorders whereas the attached article relates to the treatment of cancer. This article was published on my behalf.

I hereby disclose that all statements made herein of my own knowledge are true, and that all statements made on information and belief are believed to be true; and further that these statements are made with the knowledge that willful false statements and the like so made are punishable by fine or imprisonment, or both, under § 1001 of Title 18 of the United States Code and that such willful false statements may jeopardize the validity of the application or any patent that is issued thereon.

12 / 19 / 2005
Dated


H. Michael Shepard

Enzyme-catalyzed therapeutic agent (ECTA) design: activation of the antitumor ECTA compound NB1011 by thymidylate synthase[☆]

David B. Lackey^{a,*}, Michael P. Groziak^b, Maria Sergeeva^a, Malgorzata Beryt^c,
Christopher Boyer^a, Robert M. Stroud^d, Peter Sayre^d, John W. Park^e, Patrick Johnston^f,
Dennis Slamon^c, H. Michael Shepard^a, Mark Pegram^c

^aNewBiotics, Inc., 11760-E Sorrento Valley Rd., San Diego, CA 92121, USA

^bPharmaceutical Discovery Division, SRI International, 333 Ravenswood Ave., Menlo Park, CA 94025-3493, USA

^cUCLA School of Medicine, 10833 Le Conte Ave., Rm. 11-244, Factor Building, Los Angeles, CA 90095-1678, USA

^dUCSF, Department of Biochemistry, S-964, San Francisco, CA 94143-0448, USA

^eUCSF, 2356 Sutter St., 6th Floor, San Francisco, CA 94115, USA

^fQueens University of Belfast, Belfast, Northern Ireland BT97AB, UK

Received 21 February 2000; accepted 7 July 2000

Abstract

The *in vivo* administration of enzyme-inhibiting drugs for cancer and infectious disease often results in overexpression of the targeted enzyme. We have developed an enzyme-catalyzed therapeutic agent (ECTA) approach in which an enzyme overexpressed within the resistant cells is recruited as an intracellular catalyst for converting a relatively non-toxic substrate to a toxic product. We have investigated the potential of the ECTA approach to circumvent the thymidylate synthase (TS) overexpression-based resistance of tumor cells to conventional fluoropyrimidine [i.e. 5-fluorouracil (5-FU)] cancer chemotherapy. (*E*)-5-(2-Bromovinyl)-2'-deoxy-5'-uridyl phenyl L-methoxyalaninylphosphoramidate (NB1011) is a pronucleotide analogue of (*E*)-5-(2-bromovinyl)-2'-deoxyuridine (BVdU), an antiviral agent known to be a substrate for TS when in the 5'-monophosphorylated form. NB1011 was synthesized and found to be at least 10-fold more cytotoxic to 5-FU-resistant, TS-overexpressing colorectal tumor cells than to normal cells. This finding demonstrates that the ECTA approach to the design of novel chemotherapeutics results in compounds that are selectively cytotoxic to tumor cell lines that overexpress the target enzyme, TS, and therefore may be useful in the treatment of fluoropyrimidine-resistant cancer. © 2001 Elsevier Science Inc. All rights reserved.

Keywords: Drug resistance; Cancer; Chemotherapy; Thymidylate synthase; Phosphoramidate; Nucleoside analog

[☆]This work has been presented in preliminary form at the NCI-EORTC Symposium "Chemotherapeutic Strategies for Treatment of Colorectal Cancer: Present and Future Developments," February 10–12, 1999, Amsterdam, The Netherlands.

* Corresponding author. Tel.: +1-858-259-8600, ext. 230; fax: +1-858-259-8645.

E-mail address: dlackey1@newbiotics.com (D.B. Lackey).

Abbreviations: BVdU, (*E*)-5-(2-bromovinyl)-2'-deoxyuridine; BVdUMP, (*E*)-5-(2-bromovinyl)-2'-deoxyuridine 5'-monophosphate; NB1011, (*E*)-5-(2-bromovinyl)-2'-deoxy-5'-uridyl phenyl L-methoxyalaninylphosphoramidate; COSY, correlated spectroscopy; DCI, direct current ionization; DMF, *N,N*-dimethylformamide; dUMP, 2'-deoxyuridine 5'-monophosphate; ECTA, enzyme-catalyzed therapeutic agent; 5-FU, 5-fluorouracil; 5-FdUMP, 5-fluoro-2'-deoxyuridine 5'-monophosphate; RFU, relative fluorescence units; THF, *N*⁵,*N*¹⁰-methylene tetrahydrofolate; TBDMS, *tert*-butyldimethylsilyl; and TS, thymidylate synthase (EC 2.1.1.45).

1. Introduction

A major problem in the chemotherapeutic treatment of cancer is the development of resistance. Resistance develops when drug exposure favors the growth and reproduction of those tumor cells overexpressing enzyme(s) targeted for inhibition by the drug. For example, drug-associated enzyme overexpression in tumor cells can result from transcriptional derepression subsequent to loss of functional tumor suppressor elements such as p53, RB, and p16 [1–4]. Elevated expression also can be mediated by gene amplification *in vivo* following chemotherapy with a regimen containing 5-FU [5]. It would be particularly advantageous to capitalize on the elevated enzyme levels by administering

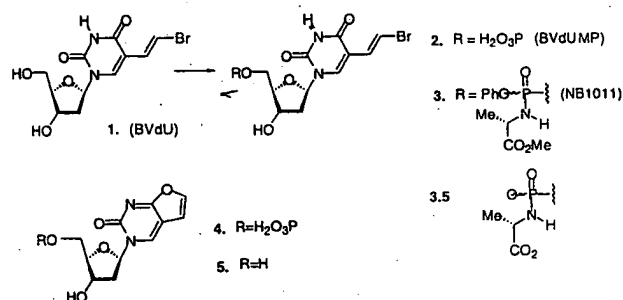


Fig. 1. Structures of pronucleotide antitumor agent NB1011 and related compounds. (1) BVdU, (*E*)-5-(2-bromovinyl)-2'-deoxyuridine; (2) BVdUMP, (*E*)-5-(2-bromovinyl)-2'-deoxyuridine 5'-monophosphate; (3) NB1011, (*E*)-5-(2-bromovinyl)-2'-deoxy-5'-uridyl phenyl L-methoxyalaninylphosphoramidate; (3.5) (*E*)-5-(2-bromovinyl)-2'-deoxy-5'-uridyl L-alaninylphosphoramidate; (4) 5,*O*4'-ethenodeoxyuridine monophosphate; and (5) 5,*O*4'-ethenodeoxyuridine.

an ECTA drug, a relatively non-toxic compound specifically designed to generate a toxic species as a result of enzymatic processing. The differential in enzyme levels between tumor (high/sensitive) and normal (low/resistant) cells should provide ECTA drugs with a beneficial therapeutic index.

TS is an enzyme critical for DNA synthesis in all organisms and is the target for both fluoropyrimidine and antifolate-based cancer chemotherapies. TS inhibitors such as 5-FU can result in more than 4-fold [6] elevation of TS, and antifolates can result in still higher levels of TS expression in tumor cells [7]. Overexpression of TS can have other consequences within cells, including suppression of p53 levels [8]. Because of the well-documented overexpression response to inhibitor drugs and the extensive background of structural and mechanistic characterization [9,10], we selected TS as the focus for the development of an ECTA approach to dealing with the problem of enzyme-mediated drug resistance.

(*E*)-5-(2-Bromovinyl)-2'-deoxy-5'-uridyl phenyl L-methoxyalaninylphosphoramidate (NB1011, 3, Fig. 1) was designed as a pronucleotide to demonstrate the ECTA concept of drug design because neutral 5'-phosphoramidates, especially phenyl L-alaninylphosphoramidate esters, are effective agents for intracellular delivery of 2',3'-dideoxyribose-based 5'-mononucleotide antiviral agents [11]. Furthermore, (*E*)-5-(2-bromovinyl)-2'-deoxyuridine 5'-monophosphate (BVdUMP, 2, Fig. 1) has been shown to be an alternative, competitive substrate for *Lactobacillus casei* TS *in vitro*, having a similar K_m but a lower k_{cat} than dUMP. By forming a covalent intermediate with 2, TS converts the inert vinylic bromide into a nucleophilic displacement-reactive allylic bromide; in the presence of 2-mercaptoethanol, this intermediate gives rise to 5-[2-(2-hydroxyethyl)thioethyl]-based dUMP derivatives in a reaction catalyzed by TS *in vitro* [12].

Based upon recent information about the active site structure of human TS [13], we predicted that the 5'-mono-

phosphate of (*E*)-5-(2-bromovinyl)-2'-deoxyuridine (BVdU, 1, Fig. 1) was likely to be converted by intracellular TS to cytotoxic reaction products without inactivating the enzyme. In addition, because TS productively binds a variety of 5'-monophosphates of uracil 2'-deoxyribonucleosides as substrates, including those with moderately sized substituents at the pyrimidine 5-position, this system offers the opportunity to explore the ECTA concept by designing and testing a variety of 5-substituted deoxyuridine derivatives.

2. Materials and methods

2.1. General methods

BVdU (1), prepared by the method of Dyer *et al.* [14], was dried *in vacuo* at 75° adjacent to P_2O_5 immediately prior to use. Radial chromatography was performed on a Chromatotron instrument (Harrison Research), using Merck silica gel-60 with a fluorescent indicator as adsorbent. BVdUMP (2) was prepared by standard chemical phosphorylation of BVdU.

2.2. NMR

1H NMR spectra were recorded on a Varian Associates Gemini spectrometer at 300 MHz, using hexadeuterio-dimethyl sulfoxide (C^2H_5) $_2SO$ solutions. Chemical shifts are reported relative to internal tetramethylsilane reference at $\delta = 0.0$ ppm. ^{13}C NMR spectra were recorded at 75 MHz, with chemical shifts reported relative to internal pentadeuterio-dimethyl sulfoxide at $\delta = 39.5$ ppm. ^{31}P NMR spectra were recorded at 202 MHz on a Bruker spectrometer, with chemical shifts reported relative to external 85% H_2O /15% H_3PO_4 , v/v, at $\delta = 0.0$ ppm.

2.3. (*E*)-5-(2-Bromovinyl)-2'-deoxy-5'-uridyl phenyl L-alaninylphosphoramidate (NB1011, 3)

A solution of 1 (420 mg, 1.26 mmol) and imidazole (103 mg, 1.51 mmol) in 2 mL of anhydrous DMF under argon was treated dropwise with phenyl L-methoxyalaninyl phosphorochloridate [15] (15 drops, 350 mg, 1.26 mmol), and the reaction mixture was stirred at 23° under argon for 24 hr. By TLC on silica gel using 10% MeOH/90% CH_2Cl_2 , v/v, as eluent, the generation of 3 ($R_f = 0.70$) from 1 ($R_f = 0.53$) had occurred but only to a partial extent (*ca.* 15%), so additional imidazole (52 mg, 0.75 mmol) and phosphorochloridate reagent (8 drops, 175 mg, 0.63 mmol) were added and the mixture was stirred at 23° under argon for another 24 hr. The solution was reduced in volume to 0.75 mL by rotary evaporation *in vacuo* at $\leq 40^\circ$, and then an equal volume of CH_2Cl_2 was added and the solution was applied directly to a dry 4-mm silica gel Chromatotron plate. Radial chromatography using 250 mL of CH_2Cl_2 (to elute residual reagents and DMF) followed by 10% MeOH/90% CH_2Cl_2 ,

v/v (to elute the product and then the starting material), gave 144 mg (20%) of **3** and 294 mg of **1**, for a 67% yield of **3** based on unrecovered **1**. If the presence of contaminating imidazole ($\delta = 7.65$ and 7.01) or DMF ($\delta = 7.95$, 2.89 , and 2.73) was detected by ^1H NMR, an additional radial chromatographic purification was performed. In this way, **3** with a purity of $\geq 98\%$ as verified by TLC and ^1H NMR was obtained as a nearly equimolar mixture of phosphorus center-based diastereomers, in oil/gum or foam-powder form: ^1H NMR $[(\text{C}^2\text{H}_3)_2\text{SO}]$ $\delta = 11.4$ (bs, exchanges with $^2\text{H}_2\text{O}$, 1, N^3H), 8.28 (pseudo-t, 1, H_6), 7.35 (pseudo-t, 2, $o\text{-Ph}$), 7.31 (d, 1, vinyl 1H), 7.20 (pseudo-t, 3, $m\text{-}$ and $p\text{-Ph}$), 6.89 (d, 1, vinyl 2H), 6.19 (t, 1, $\text{H}_{1'}$), 6.08 (t, exchanges with $^2\text{H}_2\text{O}$, 1, alaninyl NH), 5.45 (bs, exchanges with $^2\text{H}_2\text{O}$, 1, O^3H), 4.32 (m, 1, $\text{H}_{3'}$), 4.22 (m, 2, $5'\text{CH}_2$), 3.97 (m, 1, $\text{H}_{4'}$), 3.86 (t, 1, alaninyl CH), 3.58 (two s, 3, CO_2Me), 2.15 (m, 2, $2'\text{CH}_2$), 1.23 (pseudo-t, 3, alaninyl CH_3). $J_{\text{vinyl CH-vinyl CH}} = 13.5$, $J_{\text{H}_{1'}\text{-H}_{2'}} \sim 6.8$, $J_{\text{H}_{12'}\text{-H}_{13'}} \sim 5$, $J_{\text{H}_{13'}\text{-H}_{14'}} \sim 0$, $J_{\text{alaninyl CH-alaninyl NH}} \sim 6$ Hz. Spectral assignments were confirmed by $^1\text{H}/^1\text{H}$ COSY 2D NMR analysis. ^{13}C NMR $[(\text{C}^2\text{H}_3)_2\text{SO}]$ $\delta = 173.7$ and 173.6 (alaninyl CO_2), 162.1 and 161.6 (C2), 150.6 and 150.5 ($ipso\text{-Ph}$), 149.2 (C4), 139.4 and 139.2 (C6), 129.8 and 129.6 ($m\text{-Ph}$), 124.7 ($p\text{-Ph}$), 120.3 and 120.2 ($o\text{-Ph}$), 107.1 (vinyl C1), 87.5 (vinyl C2), 84.8 (C4'), 83.8 (C1'), 70.1 (C3'), 66.1 (C5'), 51.9 (alaninyl OMe), 49.7 (alaninyl $\alpha\text{-H}$), 29.5 (C2'), 19.6 (alaninyl $\alpha\text{-Me}$). $^3J_{\text{P-C4'}} = 7.8$, $^2J_{\text{P-C5'}} = 4.4$, $^2J_{\text{P-}ipso\text{-Ph}} = 6.5$ Hz. ^{31}P NMR $\delta = 3.99$, 3.69 . Low-resolution DCI (NH_3) mass: $593/591$ (MNH_4^+), $576/574$ (MH^+).

2.4. Enzyme preparation

Cloned human TS [16] was subcloned into *Escherichia coli* BL21 (DE3)/pET-28a(+) (Novagen) using the *Nde*I-*Sac*I insertion site, in order to add an amino terminal histidine tag. Enzyme was expressed in *E. coli* by induction with isopropyl β -D-thiogalactopyranoside, and purified by affinity chromatography on a Ni^{2+} His Bind metal chelation resin (Novagen). The Ni^{2+} His Bind metal chelation column was washed with 20 mM Tris (pH 7.9), 5 mM imidazole, 0.5 M NaCl; TS activity was eluted with 20 mM Tris (pH 7.9), 60 mM imidazole, 0.5 M NaCl. Purified enzyme was dialyzed against 0.5 M Tris (pH 7.5), 0.5 mM EDTA, 0.5 M NaCl and stored at -80° .

2.5. Enzyme assays

TS assays were performed in 96-well Costar UV transparent plates using a reaction volume of 200 μL , consisting of 40 mM Tris (pH 7.5), 25 mM MgCl_2 , 1 mM EDTA, 50 mM β -mercaptoethanol, 125 μM dUMP, and 65 μM THF as indicated. Tetrahydrofolate stock solutions were prepared by dissolving tetrahydrofolic acid (Sigma) directly into 0.2 M Tris (pH 7.5), 0.5 M β -mercaptoethanol; stock solutions were stored at -80° . THF was prepared by adding 12 μL of 3.8% formaldehyde to 1 mL of a 0.65 mM solution of

tetrahydrofolate and incubating for 5 min at 37° . THF was kept on ice and used within 2 hr of preparation.

Conversion of BVdUMP to fluorescent product(s) by TS was measured in 200- μL reactions containing 125 μM BVdUMP in 96-well Dynex Microfluor Black "U" bottom microtiter plates using an excitation wavelength of 340 nm and an emission wavelength of 595 nm. Reaction of BVdUMP was measured by a decrease in A_{294} . Both fluorescence and absorbance measurements were performed with a Tecan Spectrafluor Plus fluorimeter.

2.6. Cell proliferation assays

Cells growing exponentially were transferred to 384-well flat-bottom tissue culture plates. All cell types were plated at a density of 500 cells per well in 25 μL of complete medium (RPMI 1640 + 10% fetal bovine serum + antibiotics/antimycotics). After 24 hr (day 0), complete medium (25 μL) containing the experimental compounds over the concentration range of 10^{-3} to 10^{-10} M were added in triplicate wells. Drug exposure time was 120 hr (day 5), after which growth inhibition was assayed by adding 5 μL of the redox indicator, alamarBlue (Alamar, Inc.) to each well (10%, v/v). After a 4-hr incubation at 37° , fluorescence was monitored at 535 nm (excitation) and 595 nm (emission). Concentration versus relative fluorescence units (RFU) was plotted, and sigmoid curves were fit using the inhibitory E_{max} model, based on the Hill equation, in order to calculate IC_{50} directly as a parameter of the mathematical model [17].

2.7. In vivo antitumor activity of NB1011 against TS-overexpressing, 5-FU- or Tomudex-resistant human tumor xenografts

Pilot toxicology studies were performed in tumor-bearing, CD-1(nu/nu) athymic mice (Charles River Laboratories). In these studies, doses of 5 mg/mouse (250 mg/kg) given i.p. daily $\times 5$ days were well tolerated, whereas doses of 7.5 mg/mouse daily were toxic. In a 5-FU-resistant human colon carcinoma xenograft model, H630-R10 cells were injected s.c. (1.5×10^7 cells/mouse) in the mid-back region of 4- to 6-week-old athymic mice. Following 10 days to allow for tumor engraftment, six animals were assigned randomly to each treatment group, and statistical tests were performed to assure uniformity in starting xenograft volumes at the beginning of the experiment. NB1011 or control solution injections were given for 5 consecutive days. The dosages of the experimental agents were: DMSO (excipient; 40 μL), 5-FU (15 mg/kg, the MTD in this model), and NB1011 (1.25, 2.5, and 3.5 mg total dose/animal/day). Statistical analysis of the results was performed as described [18]. To confirm the findings from the colon cancer xenograft model and extend the observations to other human tumor models, a second experiment was conducted using naïve and Tomudex-resistant MCF7 human breast carcinoma xenografts (MCF7 and MCF7/TDX) grown s.c. The

xenografts were established as described above. Following 10 days to allow established xenografts to form, groups of eight mice were assigned randomly to i.p. treatment with: excipient control (DMSO), Tomudex (10 mg/kg), or NB1011 (2.5 mg/animal) days 1–5 and days 10–15. Statistical analyses of xenograft volumes were performed at the conclusion of the experiment (day 16 for MCF7/TDX and day 20 for MCF7).

2.8. Mass spectroscopy

Adherent cells growing in monolayer were washed three times with PBS at room temperature, and then were subjected to freeze/thaw lysis in 5 mL PBS. Cell extracts were centrifuged for 10 min at 8000 g; then each extract was adsorbed to a Sep-Pak Plus C₁₈ column (Millipore) and washed with 10 mL PBS. A fraction containing BVdUMP was eluted with 2 mL of distilled water. LC/MS samples were analyzed by reverse phase chromatography on a C₁₈ column using a linear gradient of 0.1% formic acid–0.1% formic acid/95% acetonitrile. Liquid chromatography response was monitored on a Micromass Quattro II triple quadrupole spectrometer. Positive ion thermospray mass spectroscopy was used to analyze reverse phase HPLC fractions of human TS enzyme reactions.

2.9. HPLC and fluorescence detection

Cells growing in 100 × 20 mm petri dishes were washed three times with PBS at room temperature, and then subjected to freeze/thaw lysis in 5 mL PBS. Cell extracts were centrifuged for 10 min at 8000 g, filtered through a 0.22 µm filter, and then passed through a 30,000 Da Amicon filter. Cell extracts were lyophilized, and then dissolved in 100 µL of distilled water. Reverse phase HPLC was performed using an Altech Adsorbosphere HS C₁₈ 5 µm column, with an HP series 1100 fluorescence detector.

3. Results

3.1. Chemical synthesis

The synthesis of NB1011 (pronucleotide 3) required the development of reaction conditions that yield primarily the 5'-phosphoramidate, while leaving the 3'-OH free. Attempts to prepare 3 along a regioselective route involving phosphoramidation of the O^{3'}-TBDMS derivatives of 1 failed when the 5'-phosphoramidate group proved sensitive to the mild conditions (tetrabutyl ammonium fluoride on silica gel, 23°, tetrahydrofuran) used to effect removal of the O^{3'} protecting group. Loss of the phosphoramidate phenoxy group was revealed by NMR. We attributed this result to intramolecular nucleophilic displacement by the 3'-hydroxyl group, suggesting a need for more acidic conditions in the synthesis of 3 (Fig. 1). Indeed, of all the nucleoside-

5'-yl phenyl L-alaninylphosphoramidates reported to date, only one—that derived from an arabinofuranoside [1-(β-D-arabinofuranosyl)-5-prop-1-ynyluracil, Netivudine]—contains a 3'-hydroxyl group [19]. We developed a direct approach that included a mild HCl scavenger in the preparation of 5'-phosphoramidates of 2'-deoxyribofuranosides as well as ribofuranosides. The regiochemical identity of 3, obtained as a 1:1 mixture of phosphorus center-based diastereomers, was firmly established by ¹H, ¹³C, and ³¹P NMR methods.

3.2. In vitro reaction of BVdUMP with human TS

Incubation of BVdUMP with TS resulted in time- and enzyme-dependent generation of fluorescence (Fig. 2A). In addition, the time-dependent increase in fluorescence was accompanied by a decrease in the BVdUMP concentration, as determined by decreasing absorbance at 294 nm (Fig. 2B). These data indicate that BVdUMP is a substrate for cloned human TS in the presence of 2-mercaptoethanol. 2-Mercaptoethanol reacted with BVdUMP to produce fluorescence in the absence of TS, but at a much slower rate (Fig. 3A). Homocysteine also supported the enzymatic conversion of BVdUMP to fluorescent product(s), but did not react with BVdUMP in the absence of TS (Fig. 3B).

Products of the reaction catalyzed by human TS with BVdUMP in a cell-free reaction have been separated by HPLC and characterized by thermospray mass spectrometry. Mass ions corresponding to predicted products of the *in vitro* TS reaction with BVdUMP in the presence of 2-mercaptoethanol were detected as possible products of the enzymatic reaction (Fig. 4). Structure I has a molecular weight of 410, and is expected (by analogy with BVdUMP and other nucleotides) to fragment by scission of the *N*-glycoside bond to yield the observed positive ion with $m/z^+ = 215$. Structure II has a molecular weight of 408, and is expected to produce the observed positive ion with $m/z^+ = 213$. Structure I corresponds to a previously characterized *in vitro* product of the *L. casei* TS reaction [12]; however, structure II, which is expected to be highly fluorescent, has not been described previously as a product of the TS reaction.

A comparison of dUMP and BVdUMP reaction characteristics is shown in Tables 1 and 2. As expected, the TS inhibitors Tomudex and 5-FdUMP inhibited enzymatic conversion of BVdUMP to fluorescent product(s) (Table 1). Conversion of BVdUMP to fluorescent product(s) by TS did not require THF, although the rate of this reaction was altered when THF was present (Table 1). Kinetic parameters for the reaction of BVdUMP catalyzed by human TS were determined using Michaelis–Menten kinetics, and are compared with the normal substrate in Table 2. Each substrate was a competitive inhibitor with respect to the other; the catalytic efficiency of BVdUMP was $4.2 \times 10^2 \text{ M}^{-1} \text{ sec}^{-1}$, whereas the catalytic efficiency of dUMP was $2.6 \times 10^4 \text{ M}^{-1} \text{ sec}^{-1}$. This indicates that dUMP was 60 times better than BVdUMP as a substrate for human TS. In contrast, *L.*

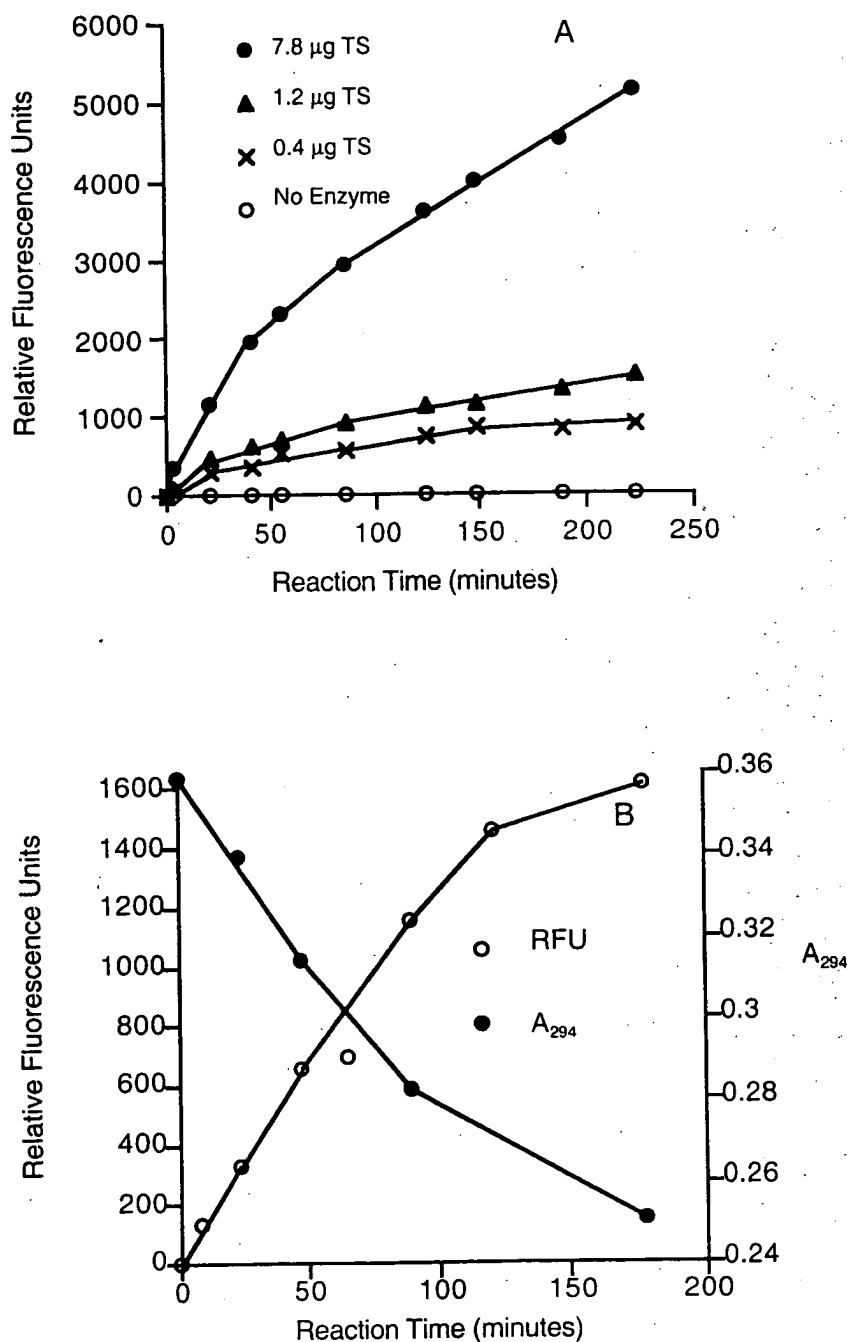


Fig. 2. Time- and enzyme-dependent generation of fluorescence catalyzed by TS. (A) BVdUMP was incubated with the indicated amounts of human TS in the standard reaction mixture at 30° (see Materials and methods), except that THF was omitted from the reaction. (B) BVdUMP was incubated with human TS in the standard reaction mixture at 30° in the absence of THF. The concentration of BVdUMP was monitored by measuring A_{294} ; fluorescence was measured as described in "Materials and methods." Each data point is the result of a single measurement.

casei TS utilizes dUMP 385 times more efficiently than BVdUMP. This latter result indicates that the substrate interaction of human TS with BVdUMP differs markedly from that of the *L. casei* TS, and suggests that BVdUMP could be an effective substrate for human TS *in vivo*.

To determine whether or not products of the reaction with BVdUMP irreversibly inhibit human TS, the enzyme

was incubated with BVdUMP for 16 hr at 30°. The amount of enzyme activity remaining after incubation was determined by measuring the oxidation of THF by monitoring absorbance at 340 nm in a standard TS assay. Preincubation of BVdUMP with the enzyme resulted in no detectable loss of activity when compared with enzyme incubated for the same length of time without BVdUMP, indicating that hu-

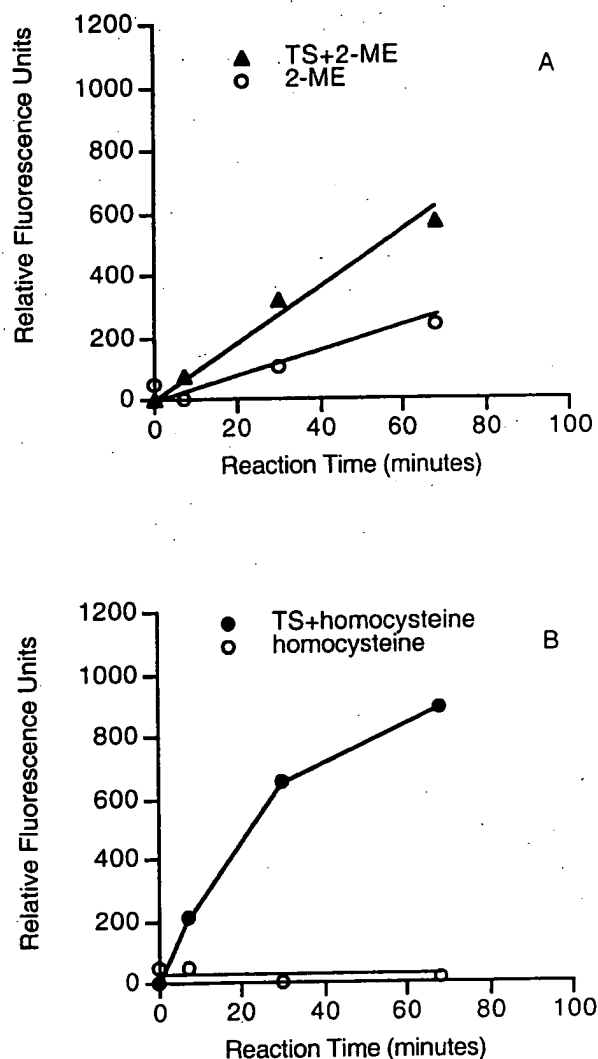


Fig. 3. Conversion of BVdUMP to fluorescent product(s) by human TS in the presence of 2-mercaptoethanol and homocysteine. (A) BVdUMP was incubated with 2-mercaptoethanol or with 2-mercaptoethanol + human TS as indicated (TS in the standard reaction mixture at 30° in the absence of THF). (B) BVdUMP was incubated with homocysteine or with homocysteine + human TS as indicated (TS in the standard reaction mixture at 30° in the absence of THF). Each data point is the result of a single measurement.

man TS is not irreversibly inhibited by BVdUMP reaction products (Fig. 5).

3.3. Intracellular formation of BVdUMP and fluorescent products from NB1011

Incubation of cells with NB1011 resulted in the accumulation of intracellular BVdUMP, as detected by LC/MS (Fig. 6). Because bromine has two naturally occurring isotopes, BVdUMP was identified readily by LC/MS as two mass ions at 411 and 413 Da with identical reverse phase chromatography retention time. The intracellular BVdUMP

concentration was measurable after as little as 14 min of incubation with 100 μ M NB1011 (Fig. 7). It should be noted that we are only measuring the net level of BVdUMP after this time; measurement of the rate of BVdUMP formation from NB1011 would have to take into account conversion of BVdUMP by intracellular enzymes, for example, conversion to BVdU by nucleotidase, and perhaps some conversion to BVdUDP and BVdUTP by kinase, as well as conversion of BVdUMP to fluorescent products by TS, and perhaps subsequent conversions to di- and triphosphates.

Combining fluorescence detection with reverse phase chromatography, we have resolved a number of fluorescent peaks that were extracted from cells after treatment with NB1011 (Fig. 8). We characterized these compounds by HPLC retention time, UV spectra, and fluorescence spectra. Treatment of NB1011 with pig liver carboxylesterase produced a compound with HPLC retention time and UV spectra identical to peak 6 (Fig. 8) by a reaction producing alaninyl BVdUMP (Fig. 1, structure 3.5) similar to the first step in the conversion of phosphoramidates to monophosphates [20]. Peak 3 was identified by retention time and UV spectra as BVdUMP (Fig. 8); peaks 1, 2, 4, and 5 had fluorescence spectra that were similar to that of the fluorescent product formed *in vitro* by the human TS reaction with BVdUMP (data not shown), although we have not yet obtained sufficient material for unambiguous structural determination.

3.4. Sensitivity of tumor cells to NB1011 *in vitro*

NB1011 was tested for cytotoxicity on a normal cell type (CCD18co) and a 5-FU-resistant tumor cell line (H630-R10), as shown in Table 3. The 5-FU-resistant tumor cell line H630-R10 was sensitive to NB1011 ($ic_{50} = 65 \pm 12 \mu$ M) in a cell proliferation assay based on reduction of the fluorescent indicator alamarBlue, whereas the normal colon cell strain CCD18co was 9-fold less sensitive to NB1011 ($ic_{50} = 562 \pm 36 \mu$ M, Table 3). Conversely, the normal CCD18co cell strain was more sensitive to 5-FU ($ic_{50} = 2.0 \pm 0.6 \mu$ M), than the drug-resistant cell line H630-R10 ($ic_{50} = 42 \pm 9 \mu$ M). Because the CCD18co cell strain was not derived from normal mucosa adjacent to the tumor from which H630-R10 was derived, this normal cell line may not be a completely fair comparison. To provide additional control experiments, we also tested H630P, the cell line that was used to select the 5-FU-resistant cell line H630-R10. H630P was slightly more sensitive to NB1011 ($ic_{50} = 433 \pm 65 \mu$ M) than the normal CCD18co cell strain. Similar results were obtained by comparing the Tomudex-resistant cell line MCF7/TDX with the Tomudex-sensitive cell line MCF7 and the normal cell line CCD18co.

We also tested a cell line containing a homozygous mutation in the TS gene, HCT C18 [21]. The HCT C18 cell

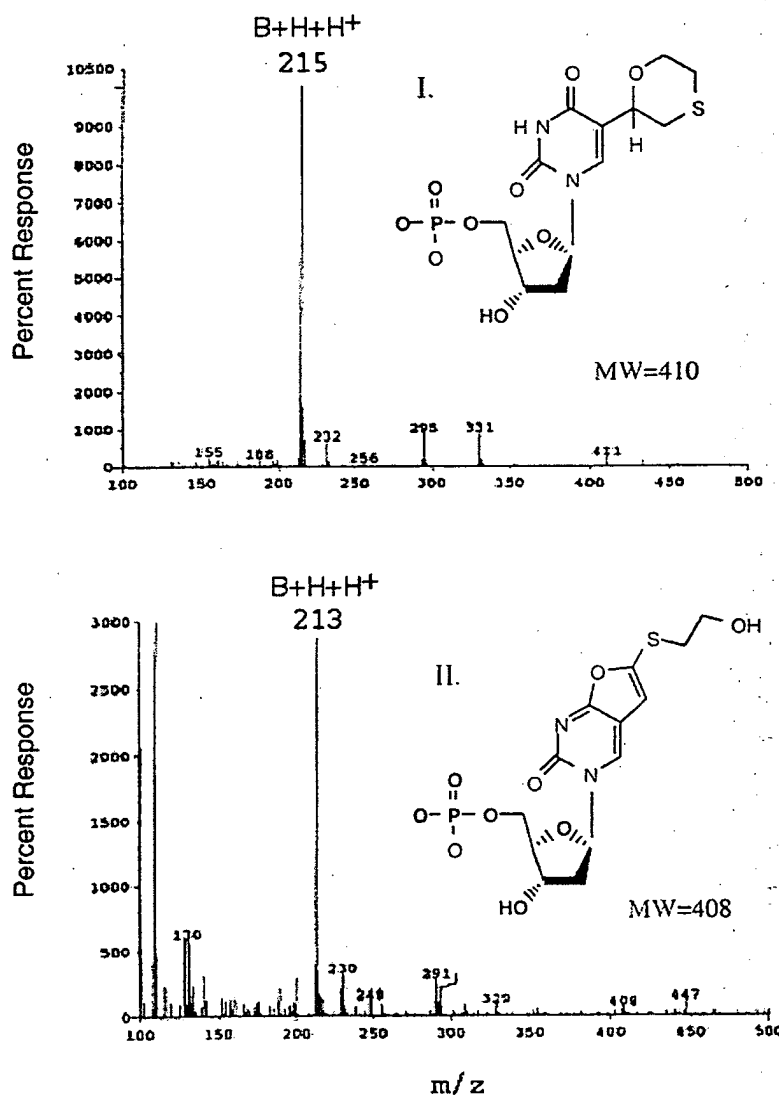


Fig. 4. Possible structures of products of *in vitro* reaction of BVdUMP catalyzed by human TS in the presence of 2-mercaptoethanol. Reaction products were isolated by reverse phase HPLC and analyzed by positive ion thermospray mass spectroscopy. The resulting m/z^+ values corresponding to the base formed by scission of the *N*-glycoside bond are consistent with structures I and II, as indicated.

line was slightly more resistant to NB1011 than the parental cell line HCT C containing a fully functional TS gene.

3.5. Sensitivity of mouse xenografts to NB1011

To extend the *in vitro* observations of cytotoxic activity of NB1011 against TS-overexpressing tumor cell lines, experiments were conducted using two different TS-overexpressing human tumor xenograft models *in vivo*. In the first experiment, 5-FU-resistant, human colon cancer cells (H630-R10) were grown s.c. in athymic mice. Animals were treated with NB1011, 5-FU, or excipient (Fig. 9A). There was complete suppression of xenograft growth in the NB1011 groups versus the 5-FU or excipient-treated controls during treatment with NB1011 (days 1–5, Fig. 9A). This significant difference ($P < 0.05$) was maintained

Table 1
Inhibition of human TS reactions by Tomudex™ and 5-FdUMP

Substrate ± cofactor	Reaction rate		
	No inhibitor	Tomudex™ (500 nM)	5-FdUMP (500 nM)
BVdUMP + THF	109 ± 16 RFU/min (100%)	67 ± 3 (61%)	44 ± 2 (40%)
BVdUMP – THF	75 ± 11 (100%)	34 ± 3 (45%)	93 ± 13 (129%)
dUMP + THF	1500 ± 20 nmol/min (100%)	690 ± 40 (46%)	290 ± 70 (19%)

TS reactions containing enzyme inhibitors were incubated at 30° as described in "Materials and methods," and the initial rates of the enzyme reaction were determined by measuring the increase in A_{340} . Conversion of BVdUMP to a fluorescent product(s) was measured using 340 nm excitation and 595 nm fluorescence emission. Values are means ± SD, $N = 3$.

Table 2
Enzyme kinetic constants for human and *Lactobacillus* TS

Nucleotide	Kinetic constants	<i>L. casei</i> ^a	<i>Homo sapiens</i>
dUMP	K_m	3.0 μM	7.7 μM
	k_{cat}	6.4 sec^{-1}	0.2 sec^{-1}
	k_{cat}/K_m (catalytic efficiency)	$2.1 \times 10^6 \text{ M}^{-1} \text{ sec}^{-1}$	$2.6 \times 10^4 \text{ M}^{-1} \text{ sec}^{-1}$
	K_i	0.6 μM	17.5 μM
BVdUMP	K_m	3.3 μM	16 μM
	k_{cat}	0.018 sec^{-1}	0.0067 sec^{-1}
	k_{cat}/K_m (catalytic efficiency)	$5.5 \times 10^3 \text{ M}^{-1} \text{ sec}^{-1}$	$4.2 \times 10^2 \text{ M}^{-1} \text{ sec}^{-1}$
	K_i	2.0 μM	4.5 μM
dUMP catalytic efficiency/ BVdUMP catalytic efficiency		385-fold	60-fold

Initial rates for enzyme reactions containing dUMP were determined by measuring the increase in A_{340} . The rate of reactions containing BVdUMP was determined by measuring the decrease in A_{294} , as described in "Materials and methods."

^a Data from Ref. 12.

through the end of the experiment (day 26; Fig. 9A, inset). To confirm the findings from the 5-FU-resistant, TS-overexpressing colon cancer xenograft model, and to extend our observations into other xenograft models, further experimentation was performed using naïve and Tomudex-resistant, TS-overexpressing human breast cancer xenografts (MCF7 and MCF7/TDX). In both models, treatment with NB1011 resulted in decreased xenograft volume (compared with day 1) in five of eight treated animals, including one complete response by day 17 (MCF7/TDX, Fig. 9B). The average NB1011-treated MCF7 or MCF7/TDX xenograft volume was also significantly less than excipient-treated controls ($P < 0.05$), whereas Tomudex-treated xenografts were not significantly different from excipient-treated controls ($P = 0.30$). Treatment of non-selected MCF7 tumors gave similar results (Fig. 9C).

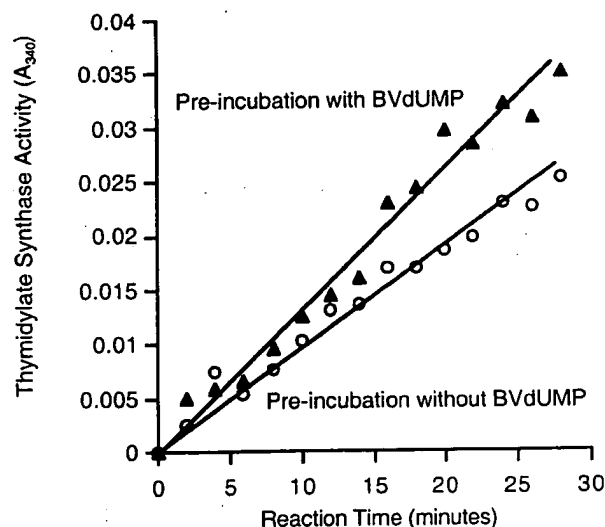


Fig. 5. Effect of preincubation of human TS with BVdUMP. Human TS was preincubated with and without BVdUMP for 16 hr in the absence of THF. Remaining enzyme activity was measured by adding dUMP and THF and measuring absorbance at 340 nm as described in "Materials and methods." Each data point is the result of a single measurement.

4. Discussion

The LC/MS analysis of cell extracts, combined with HPLC fluorescence detection and UV spectra, demonstrated that NB1011 treatment results in the appearance of BVdUMP in cell extracts. In addition, a number of fluorescent products were detected in extracts prepared from cells treated with NB1011. We suggest that the selective tumor cell cytotoxicity of NB1011 may be due, at least in part, to the eventual production of compounds similar to 4 (Fig. 1), a 5,*O*⁴-ethenodeoxyuridine nucleotide. The TS-dependent

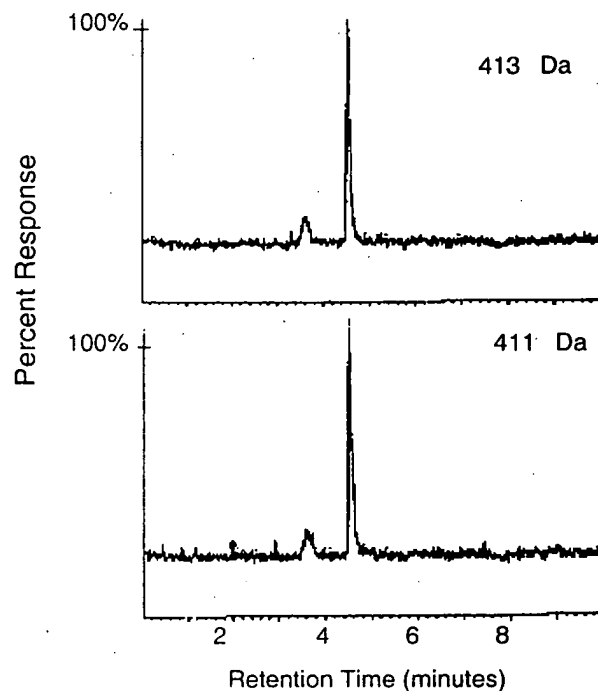


Fig. 6. LC/MS detection of intracellular BVdUMP. H630-R10 cells were treated with 100 μM NB1011 for 5 days, and cell extracts were prepared for LC/MS as described in "Materials and methods." Control extracts prepared from untreated cells were analyzed at the same time, and showed no mass ion corresponding to BVdUMP.

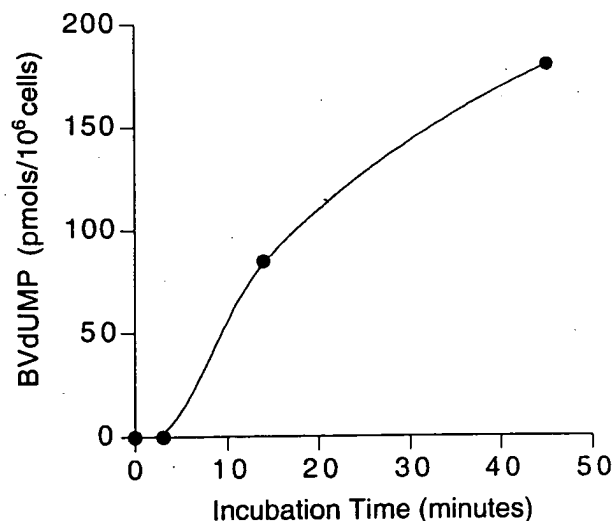


Fig. 7. Time course of accumulation of intracellular BVdUMP. H630-R10 cells were treated with 100 μ M NB1011 for the indicated time. Extracts were prepared and analyzed by LC/MS as described in "Materials and methods." Each time point is the result of a single measurement.

intracellular production of **4** might proceed by dehydration of a dUMP-5-acetaldehyde TS product that would arise if water reacted with the TS-bound allylic bromide intermediate, or by direct intramolecular displacement of this bromide by the deoxyuridine O⁴ atom while still within the TS active site. These reactions have a strong precedent in a chemical model reaction, namely, the generation of the parent heterocycle furano[2,3-*d*]pyrimidin-2(3*H*)-one itself in an 89% yield when 5-(2-bromovinyl)uracil is treated with

Table 3
Sensitivity of cell lines to NB1011, 5-FU, and TomudexTM

Cell line	NB1011 IC ₅₀ (μ M)	5-FU IC ₅₀ (μ M)	TDX IC ₅₀ (nM)
CCD18co	562 \pm 36	2.0 \pm 0.6	20 \pm 5
H630P	433 \pm 65	2.1 \pm 0.3	6.2 \pm 1
H630-R10	65 \pm 12	42 \pm 9	330 \pm 17
MCF7P	207 \pm 26	1.0 \pm 0.1	1.8 \pm 0.1
MCF7/TDX	3 \pm 2	6.0 \pm 1.2	>1000
HCT C TS ⁺	281 \pm 27	2.8 \pm 0.1	ND
HCT C18 TS ⁻	348 \pm 55	3.6 \pm 0.5	ND

H630-R10 and MCF7/TDX cell lines were selected for resistance to 5-FU and TomudexTM, respectively, as described in "Materials and methods". The IC₅₀ values were determined as described in "Materials and methods"; ND indicates that the assay was not done. Values are means \pm SEM, N = 3.

base [22]. In addition, similar heterocycles are produced in 61–65% yields by the condensation of 5-allyl-6-chloro-1-methyluracil and amines [23].

A 5, O⁴-ethenodeoxyuridine nucleotide similar to **4** is expected to be fluorescent by analogy to 3, N⁴-ethenodeoxycytidine and by structural similarity to the fluorescent furano[2,3-*d*]pyrimidin-2(3*H*)-one nucleoside byproducts that form during the Heck-type coupling of 5-halo-2'-deoxyuridines and ethynes [24]. The nucleoside **5** has been synthesized; this compound has a fluorescence emission maximum of 400 nm.¹ In addition, the *in vitro* processing of

¹ Castillo R and Chan F. Personal communication. Cited with permission.

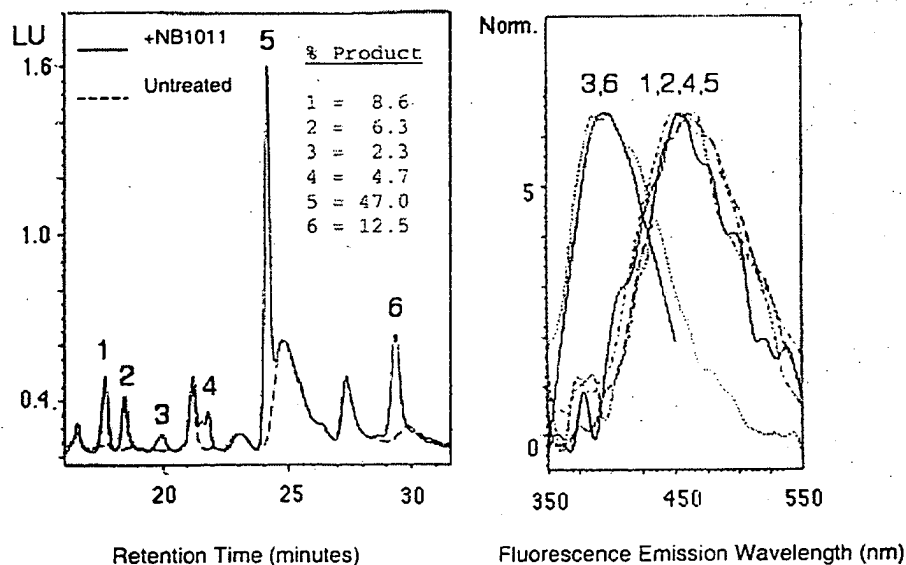


Fig. 8. Detection of intracellular fluorescent products after treatment of RKO cells with NB1011. Cell extracts from NB1011-treated and control cells were prepared and analyzed on C₁₈ reverse phase HPLC as described in "Materials and methods." Peaks were detected by fluorescence (excitation 320 nm/emission 450 nm); peaks present in NB1011-treated cell extracts but not present in extracts from untreated cells are labeled 1 through 6 in order of increasing retention time. The inset lists the percent of total fluorescence for peaks 1–6.

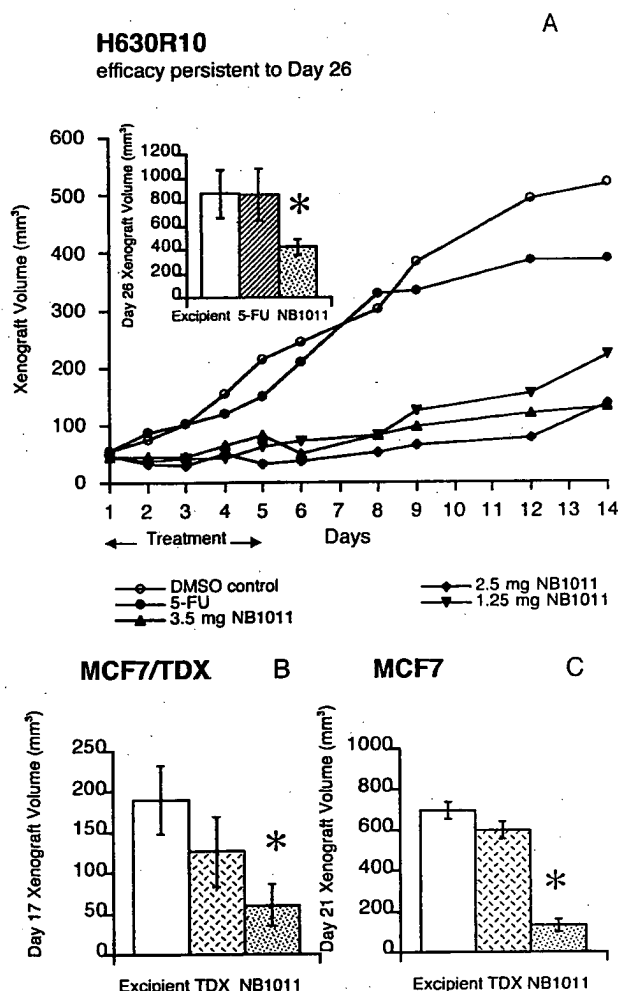


Fig. 9. Effect of NB1011 on drug-resistant colon and breast cancer *in vivo*. (A) Treatment of athymic mice bearing H630-R10 (5-FU resistant) human colon carcinoma. Inset: Long-term response to NB1011—analysis of pooled data at day 26. (B) Tomudex-resistant MCF7/TDX breast carcinoma. Statistical analysis is described in "Materials and methods." (C) Non-selected MCF7 tumors. An asterisk (*) indicates statistically significant tumor suppression as compared with either 5-FU or Tomudex-treated animals, $P < 0.05$. Values are means \pm SEM, $N = 6$.

BVdUMP by TS proceeds with the generation of a fluorescent compound(s) in the presence of 2-mercaptoethanol and homocysteine. Analysis by mass spectroscopy of human TS products obtained from reactions containing BVdUMP and 2-mercaptoethanol is consistent with a fluorescent product (structure II, Fig. 4). This compound may be a previously undescribed fluorescent product of the human TS reaction; a complete structural analysis of these products is underway. The multiple fluorescent peaks obtained by reverse phase chromatography of NB1011-treated cell extracts may represent products obtained by TS-catalyzed reaction of BVdUMP with intracellular thiols. For example, homocysteine can participate in an *in vitro* reaction catalyzed by human TS that converts BVdUMP to a fluorescent product(s) (Fig. 3B).

Our results clearly show that a TS ECTA approach can be successful for selectively targeting colorectal tumor cells that overexpress TS. The most likely products of this reaction are unusual nucleoside monophosphates that may have multiple intracellular targets; we have not detected the corresponding intracellular nucleoside di- and triphosphates using analytical HPLC. Furthermore, using an analytical HPLC method for determining base composition that is capable of detecting minor DNA bases such as 5-methylcytosine, we have not detected additional bases in DNA or RNA following NB1011 treatment. Although we have not yet determined precisely which TS catalyzed products arising from NB1011 are responsible for the selective tumor cell cytotoxicity of NB1011, these results provide a strong rationale for using the TS ECTA approach to design a new generation of therapeutic agents that are activated by TS and other drug resistance-associated intracellular enzymes.

The possible clinical application of TS ECTA compounds is supported further by treatment of human colon (H630-R10; 5-FU resistant) and breast (MCF7 and MCF7/TDX) cancers in athymic mice. NB1011 caused growth inhibition and tumor regressions in all three models. This result is predicted for the two tumor types expressing high levels of TS (H630-R10 and MCF7/TDX). The activity of NB1011 against unselected MCF7 breast cancer is a possible function of the fact that *in vivo*, where normal cell growth constraints are in place, the MCF7 tumor cells express a higher level of TS than normal tissues. The lack of toxicity of the compound within the therapeutic range (1.25 to 3.5 mg/animal/day) further supports the selectivity of NB1011.

References

- [1] Lee Y, Chen Y, Chang LS, Johnson LF. Inhibition of mouse thymidylate synthase promoter activity by the wild-type p53 tumor suppressor protein. *Exp Cell Res* 1997;234:270–6.
- [2] Almasan A, Linke SP, Paulson TG, Huang LC, Wahl GM. Genetic instability as a consequence of inappropriate entry into and progression through S-phase. *Cancer Metastasis Rev* 1995;14:59–73.
- [3] Bjornland K, Winberg JO, Odegard OT, Hovig E, Loennechen T, Aasen AO, Fodstad O, Maelandsmo GM. S100A4 involvement in metastasis: deregulation of matrix metalloproteinases and tissue inhibitors of matrix metalloproteinases in osteosarcoma cells transfected with an anti-S100A4 ribozyme. *Cancer Res* 1999;59:4702–8.
- [4] Li W, Fan J, Hochhauser D, Banerjee D, Zielinski Z, Almasan AY, Kelly R, Wahl GM, Bertino JR. Lack of functional retinoblastoma protein mediates increased resistance to antimetabolites in human sarcoma cell lines. *Proc Natl Acad Sci USA* 1995;92:10436–40.
- [5] Lonn U, Lonn S, Nilsson B, Stenkvist B. Higher frequency of gene amplification in breast cancer patients who received adjuvant chemotherapy. *Cancer* 1996;77:107–12.
- [6] Peters GJ, van der Wilt CL, van Triest B, Codacci-Pisanelli G, Johnston PG, van Groeningen CJ, Pinedo HM. Thymidylate synthase and drug resistance. *Eur J Cancer* 1995;31A:1299–305.
- [7] Jackman AL, Kelland LR, Kimbell R, Brown M, Gibson W, Aheme GW, Hardcastle A, Boyle FT. Mechanisms of acquired resistance to the quinazoline thymidylate synthase inhibitor ZD1694 (Tomudex) in one mouse and three human cell lines. *Br J Cancer* 1995;71:914–24.

- [8] Ju J, Pedersen-Lane J, Maley F, Chu E. Regulation of p53 expression by thymidylate synthase. *Proc Natl Acad Sci USA* 1999;96:3769–74.
- [9] Carreras CW, Santi DV. The catalytic mechanism and structure of thymidylate synthase. *Annu Rev Biochem* 1995;64:721–62.
- [10] Montfort WR, Weichsel A. Thymidylate synthase: structure, inhibition, and strained conformations during catalysis. *Pharmacol Ther* 1997;76:29–43.
- [11] Balzarini J, Cahard D, Wedgwood O, Salgado A, Velázquez S, Yarnold CJ, De Clercq E, McGuigan C, Thormar H. Marked inhibitory activity of masked aryloxy aminoacyl phosphoramidate derivatives of dideoxynucleoside analogues against visna virus infection. *J Acquir Immune Defic Syndr Hum Retrovirol* 1998;17:296–302.
- [12] Barr PJ, Oppenheimer NJ, Santi DV. Thymidylate synthetase-catalyzed conversions of *E*-5-(2-bromovinyl)-2'-deoxyuridylate. *J Biol Chem* 1983;258:13627–31.
- [13] Schiffer CA, Clifton IJ, Davisson VJ, Santi DV, Stroud RM. Crystal structure of human thymidylate synthase: a structural mechanism for guiding substrates into the active site. *Biochemistry* 1995;34:16279–87.
- [14] Dyer RL, Jones AS, Walker RT. Nucleic acid chemistry. Improved and new synthetic procedures, methods, and techniques. New York: Wiley-Interscience, 1991.
- [15] McGuigan C, Pathirana RN, Mahmood N, Devine KG, Hay AJ. Aryl phosphate derivatives of AZT retain activity against HIV1 in cell lines which are resistant to the action of AZT. *Antiviral Res* 1992;17:311–21.
- [16] Davisson VJ, Sirawaraporn W, Santi D. Expression of human thymidylate synthase in *Escherichia coli*. *J Biol Chem* 1989;264:9145–8.
- [17] Levasseur LM, Slocum HK, Rustum YM, Greco WR. Modeling of the time-dependency of *in vitro* drug cytotoxicity and resistance. *Cancer Res* 1998;58:5749–61.
- [18] Pegram M, Hsu S, Lewis G, Pietras R, Beryt M, Sliwkowski M, Coombs D, Baly D, Kabbinnavar F, Slamon D. Inhibitory effects of combinations of HER-2/*neu* antibody and chemotherapeutic agents used for treatment of human breast cancers. *Oncogene* 1999;18:2241–51.
- [19] McGuigan C, Perry A, Yarnold CJ, Sutton PW, Lowe D, Miller W, Rahim SG, Slater MJ. Synthesis and evaluation of some masked phosphate esters of the anti-herpesvirus drug 882C (netivudine) as potential antiviral agents. *Antiviral Chem Chemother* 1998;9:233–43.
- [20] Saboulard D, Naesens L, Cahard D, Salgado A, Pathirana R, Velázquez S, McGuigan C, De Clercq E, Balzarini J. Characterization of the activation pathway of phosphoramidate triester prodrugs of stavudine and zidovudine. *Mol Pharmacol* 1999;56:693–704.
- [21] Hoganson DK, Williams AW, Berger SH. Isolation and characterization of a thymidylate synthase-deficient human colon tumor cell line. *Biochem Pharmacol* 1999;58:1529–37.
- [22] Eger K, Jalalian M, Schmidt M. Steric fixation of bromovinyluracil: synthesis of furo[2,3-*d*] pyrimidine nucleosides. *J Heterocycl Chem* 1995;32:211–8.
- [23] Ishikawa I, Kachatrian VE, Melik-Ohanjanian RG, Kawahara N, Mizuno Y, Ogura H. Synthesis of 7-alkyl-1,3,6-trimethylpyrrolo[2,3-*d*]pyrimidines and 4-alkylamino-2,5-dimethyl-2,3-dihydrofuro[3,2-*e*]pyrimidines. *Chem Pharm Bull (Tokyo)* 1992;40:846–50.
- [24] Robins MJ, Barr PJ. Nucleic acid related compounds. 39. Efficient conversion of 5-iodo to 5-alkynyl and derived 5-substituted uracil bases and nucleosides. *J Org Chem* 1983;48:1854–62.

**This Page is Inserted by IFW Indexing and Scanning
Operations and is not part of the Official Record**

BEST AVAILABLE IMAGES

Defective images within this document are accurate representations of the original documents submitted by the applicant.

Defects in the images include but are not limited to the items checked:

☒ **BLACK BORDERS**

☐ **IMAGE CUT OFF AT TOP, BOTTOM OR SIDES**

☒ **FADED TEXT OR DRAWING**

☒ **BLURRED OR ILLEGIBLE TEXT OR DRAWING**

☐ **SKEWED/SLANTED IMAGES**

☐ **COLOR OR BLACK AND WHITE PHOTOGRAPHS**

☐ **GRAY SCALE DOCUMENTS**

☐ **LINES OR MARKS ON ORIGINAL DOCUMENT**

☐ **REFERENCE(S) OR EXHIBIT(S) SUBMITTED ARE POOR QUALITY**

☐ **OTHER:** _____

IMAGES ARE BEST AVAILABLE COPY.

As rescanning these documents will not correct the image problems checked, please do not report these problems to the IFW Image Problem Mailbox.